Türkiye Jeoloji Bülteni
Geological Bulletin of Turkey
65 (2022) 159—170
doi: 10.25288/tjb.1035354

Geophysical Study to Identify Iron Mineralization Anomalies Using Terrestrial Magnetometry in the Chak-Chak Exploration Area, Iran

Ali Akbar Aali[1], Aref Shirazi[1], Adel Shirazy[1*], Shayan Khakmardan[1,2], Abbas Maghsoudi[1], Ardeshir Hezarkhani[1]

[1] *Faculty of Mining Engineering, Amirkabir University of Technology (Tehran Polytechnic), Tehran, Iran.*
[2] *École Nationale Supérieure de Géologie, University of Lorraine, Lorraine, France*

• Geliş/Received: 10.12.2021 • Düzeltilmiş Metin Geliş/Revised Manuscript Received: 17.01.2022 • Kabul/Accepted: 21.02.2022
• Çevrimiçi Yayın/Available online: 23.03.2022 • Baskı/Printed: 15.04.2022

Araştırma Makalesi/Research Article *Türkiye Jeol. Bül. / Geol. Bull. Turkey*

Abstract: Abstract: Mineral exploration is the underlying theme of industry and discoveries because humans have been exploring for minerals from the very beginning, based on their needs. This research aims to find promising areas of iron ore mineralization in Chak-Chak Exploration area of Yazd province, Iran. The study's range lies at a latitude of 32-33 degrees north and a longitude of 54-55 degrees east. This study collected data using terrestrial magnetometry at 6222 points in a 20 m x 10 m grid. Initially, these data were pre-processed, such as removing the magnetic field effect of the Earth's core. Subsequently, processes such as applying polarisation filters, trend surface correction, upward and downward conversions, vertical derivatives and analytical signals on the terrestrial magnetic data were performed. The Exploration range contains numerous peaks in the southwest and other summits in the northeast, according to the research findings. These anomalies are consistent with igneous rock units (rhyolites) and faults. Consequently, it may be stated that one of the most rapid and least costly methods of detecting iron anomalies is terrestrial magnetism, which produces satisfactory results.

Keywords: Chak-Chak, iron, magnetic field, mineralization, terrestrial magnetism.

INTRODUCTION

In recent years, many methods have been used to explore for mineral deposits, by using geochemistry, geophysics and remote sensing (Shirazi et al., 2018a & 2018c; Shirazy et al., 2021b, 2021c & 2021e). One of the geophysical methods in the exploration of deposits is the magnetometric method (Khayer et al., 2021; Shirazy et al., 2021a & 2021d), and it has been used for many years to explore for economic minerals such as iron and oil. Study of the Earth's magnetic field has been carried out since William Gilbert (1544-1603). However, Johannes Diderik van der Waals (1837-1923) was the first to determine the location of magnetic deposits with the help of changes in the Earth's magnetic field (Chelotti et al., 2009). Along with growing demand in the metals market and the increasing use of fossil fuels, geophysical exploration methods, including magnetometry, became very important. The reason for the importance of the magnetometric method is that the magnetometer can test a wide area at a lower cost (Shirazy et al., 2020a, 2020b & 2021d; Tian et al., 2010;).

The magnetometric method is used to identify subsurface properties of the Earth from the point

* Correspondence / *Yazışma*: adel.shirazy@aut.ac.ir

of view of magnetic field anomalies (Nabighian et al., 2005; Shirazy et al., 2018a, 2018b & 2022). These anomalies originate from the magnetic properties of subsurface rock units. Although only a limited number of rock forms have magnetic properties, this limited number of minerals with magnetic properties has led to significant magnetic anomalies. Accordingly, magnetometry has many applications (Khosravi et al., 2022; Liu et al., 2017). This method has been used on a small scale for engineering and archaeological studies to identify metal objects, and on a large scale for geological studies. Magnetic measurements can be applied to the air, land and sea and have been used in various fields (Edelstein, 2007; Khayer et al., 2021).

In general, materials are divided into three categories regarding their presence in the magnetic field (Spaldin, 2010): diamagnetic, paramagnetic and ferromagnetic. Diamagnetic materials have negative self-adhesion. Paramagnetic materials have weak positive self-acceptance, and ferromagnetic materials have solid and positive self-acceptance. Iron oxides, which are ferromagnetic minerals, are the main target of magnetometric discoveries. Minerals with high magnetic properties affect the Earth's magnetic field. Protons or caesium vapours are some of the devices used to measure the Earth's magnetic field with nanotesla accuracy. The Earth's magnetic field is the sum of regional fields and local anomalies. Induction magnetism is obtained in the presence of a magnetic field according to Equation (1) (Currenti et al., 2007):

$$J=KH \quad (1)$$

In this sense, H refers to the magnetic field in terms of tesla, K represents the magnetic resistivity, a unitless parameter, and J is the induction magnet in ampere meters (Shirazi et al., 2018a & 2018b; Shirazy et al., 2021b & 2021c).

The leading cause of magnetic anomalies in rocks are dykes, faults, folds, sills, metamorphic fundamental rocks and magnetite deposit masses. In general, all magnetic minerals lose their magnetic properties at roughly 600 degrees Celsius (Edelstein, 2007; Shirazy et al., 2020a & 2020b). About 90% of iron deposits comes from sedimentary deposit types, and the 10% remaining come from mafic, ultramafic and skarn igneous deposits. In igneous rocks, the ratio of hematite to magnetite is higher than other rocks and therefore, it is easily recognized by the terrestrial magnetometry method (Dobrin & Savit, 1988; Doodran et al., 2020; Khakmardan et al., 2020).

In the exploration of mineral deposits, magnetometry is often used as a direct measurement. When magnetic measurements are made directly for identifying magnetic minerals, non-magnetic minerals are also detected (Abubakar et al., 2015; Shirazy et al., 2021a, 2021b & 2021c). With the help of advanced tools, it is possible to measure very little of the magnetic field's magnitude in sedimentary rocks near the Earth's surface. The terrestrial magnetometric method is a type of magnetometric method. The terrestrial magnetometry is performed in small pre-defined areas. The distance between the measuring points in this method is between 10 and 100 meters. However, in areas with strong magnetic gradients, this distance is reduced. In order to apply the terrestrial magnetometer method, proximity to railways, cars, roads, fences, and anything else that might affect the local magnetic field should be avoided. Fluxgate and proton magnetometers are among the devices used to measure the Earth's magnetic field. Because advanced magnetometers do not require precise alignment, so a terrestrial magnetometric operation is always much faster than the gravimetry method (Minshull, 2003; Shirazi et al., 2018b, & 2018c; Shirazy et al., 2019 &, 2021d).

Due to the importance of the magnetometric method in exploring for iron ore, the terrestrial magnetometry method was used to determine areas with iron anomalies in the area of Chak-

Chak Exploration area in Yazd province in this study. The study area is located to the north of Chak-Chak Exploration area and the southwest of Toot/Tut village. Access to the area consists of a 67 km asphalt road from Ardakan city to Toot village and then 8 km of dirt road between this village and the study area. The coordinates are between 250200 to 252400 m longitude and 3595300 to 3597000 m latitude, and the average height is 1730 meters in the UTM system. Figure 1 shows the roadmap for access to the study area. This study aims to find anomalous points and investigate the mineralization potential in this area using terrestrial magnetometric data. It is projected that the search for iron anomalies will continue throughout the exploratory stages.

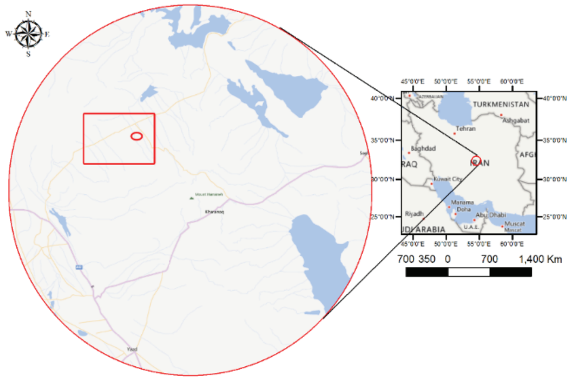

Figure 1. Geo-location of study area on Iran map.

GEOLOGY of the EXPLORATORY AREA

The study area is located in Yazd province, Iran, around Chak-Chak Exploration area. Chak-Chak Exploration area is located 47 km east of Ardakan. The study area further covers new alluviums, altered rhyolites, weathered feldspars, and a few diabase outcrops. These rocks are mainly found with oxidative impurities. Diabase extrusions with iron oxide impurities and subvolcanic rocks such as quartz monzonite can be seen in some parts of the area. Andesitic tuffs and weathered rhyolites cover the vast area. Silica veins with low to medium thickness are present in the western regions of the area. The texture of the stones in the area is microporphyry. In the region's rocks, there are metallic minerals such as pyrite, chalcopyrite, hematite, iron hydroxide and titanium oxide (Alahgholi et al., 2018; Company, 2018; Khakmardan et al., 2018; Shirazi et al., 2018d). A geological map of the exploratory area is shown in Figure 2.

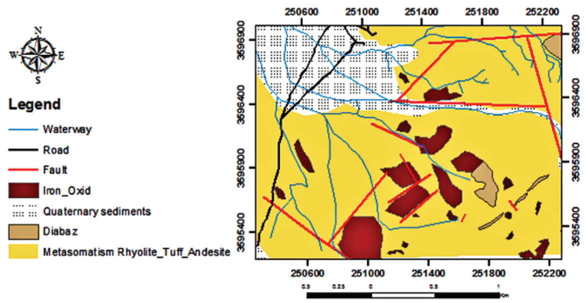

Figure 2. Geological map of study area.

The study regions of the Exploration area is located in the Ziroo Formation (Ghorbani, 2013b). Lithologically, this formation has pyroclastic, volcanic and volcanoclastic rocks. Based on stratigraphic observations, the age of rock units in this range has been estimated as Lower Precambrian. The study area is composed of metamorphic volcanic and volcanoclastic rocks to the extent of rhyolite and rhyolite tuff. Metamorphic black clastic rocks are also observed in the study area. Alluvial sediments in the form of basins and old alluvial fans cover some parts of the area. The age of alluvial sediments is within the Quaternary era (Company, 2016; Ghorbani, 2013a; Shirazy et al., 2018a, 2018b & 2021b).

NETWORK GRID DESIGN

According to the tendancy of geological structures in the area and previous studies, as well as some excavated trenches and the employer's opinion, the measurement grid network was designed with a north-south profile, as can be seen in Figure 3. In this area, 6222 points in a network with dimensions of 20 by 10 meters were measured by Yaghoot Zafar Yazd Cooperative Company during two stages in the author's presence. A distance of 20 meters between pick-up profiles and 10 meters between pick-up points was considered appropriate for each profile. The reason for choosing these dimensions for the selected grids in the networks was the presence of small masses of iron under the sediments, which were searched using this network with maximum sensitivity.

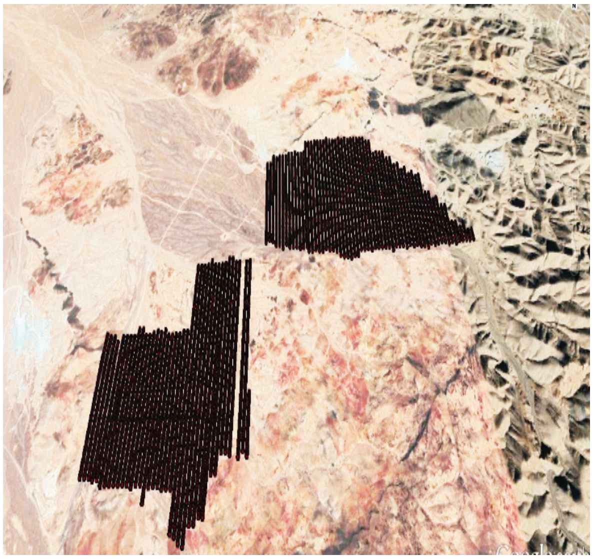

Figure 3. Pick-up designed grid for magnetometric data in study area.

This project's magnetic data measurement was conducted with a Proton Precession magnetometer GSM-19T, the latest model of the company GEM in Canada (Bao-xian, 2013). Unlike a fluxgate magnetometer, these types of magnetometers can only measure the magnitude of the Earth's total magnetic field. The cylindrical tank, which is filled with a liquid saturated with hydrogen atoms and wrapped around a coil, forms the sensitive part of the device. With its many advantages and the use of proton precision technology, this device has made many advances in Earth sciences. This device has high precision selectivity in magnetic anomaly separation with a magnetic resolution of 0.01 nanotesla.

Figure 4 shows the measurement network grid in the Exploration area and a magnetic map of the entire range. Data measurement was performed on two different ranges. According to Figure 4, the minimum magnetic field strength in one range is 43362 nanotesla, and the maximum magnetic field strength is 52801 nanotesla. The maximum change in the magnetic field of the other range is 9439 nanotesla.

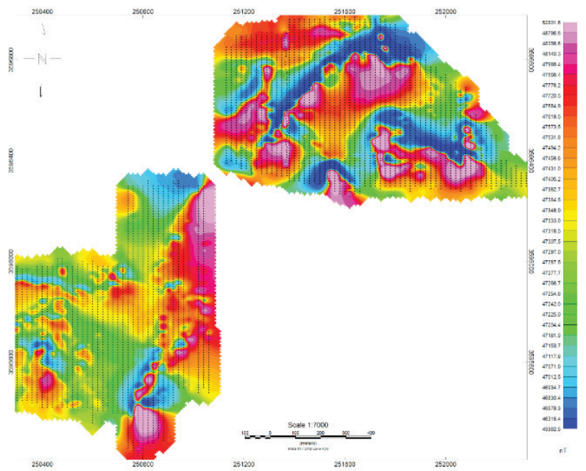

Figure 4. View of measurement grid in range with magnetometric map of entire range.

DATA PREPROCESSING

Data processing was performed using Geosoft Oasis montaj 6.4.2 software. The magnetic value at the base station must be measured before each reading to correct the magnetic data. In the next step, the magnetometer is placed on the base point, and another device does the daily reading of the stations. After making the measurements, the data is discharged from the device and forms databases in the software. This data is used to correct and process the data.

The first step in preprocessing terrestrial magnetometric data is the daily correction. Daily changes have a periodicity and intermittently affect phenomena, such as tides. The maximum range of daily change effects is 50 nanotesla per day. These changes can be eliminated in several ways. The second preprocessing operation is latitude and longitude correction. One of the critical points in magnetometric data is that latitude and longitude are not very effective in the measurement of data. The vertical gradient of the total field varies from an approximate maximum of 0.1 gamma per foot at the Earth's poles to a minimum of 0.005 gamma per foot at the magnetic equator. The variation of the magnetic field between the equator and the poles is more than ten gamma. Therefore, there is no need for magnetic corrections related to latitude.

On the other hand, due to the location of Iran, the magnetic changes along the geographical longitude is negligible, and therefore, there is no need to make this correction. Height correction is the third preprocessing step on the terrestrial magnetometric data. Topography can have a significant effect on terrestrial magnetometric data. This correction in the exploration of ferromagnetic minerals, where the field changes are substantial, is not required, but should be considered in cases where small amounts of magnetic field influence decisions. In this project, the amount of the topographic effect on the magnetic data was insignificant, so this correction was not performed. Finally, the effect of the Earth's magnetic field must be normalized. To prepare magnetic field anomaly maps, one must first calculate the effects of the magnetic field on the Earth's core by considering the international geomagnetic reference field (IGRF) values and subtracting them from the data. The result of this operation is the residual values related to the anomalies in the Exploration area. Then, in order to prepare the anomaly map, the total magnetic field data of the range is networked.

The entire magnetic field map of the study area after daily correction is presented in Figure 5. In order to remove the Earth's core magnetic field effect, the IGRF effect was calculated and reduced in the exploratory range where the magnetometric data was collected. The IGRF effect map and the entire magnetic field map of the study area, after removing the IGRF effect, are presented respectively in Figures 6 and 7. According to Figure 7, the area has several maxima in the southwest (anomalies A, B, C and D) and other peaks in the northeast (anomalies E, F, G, H, and I). These anomalies correspond to the igneous rock units (rhyolites) and faults of the Exploration area. A dipole is located in the central part of the range, which is unreliable due to incomplete data, and must be processed and interpreted after measurement of the surrounding data (anomaly D).

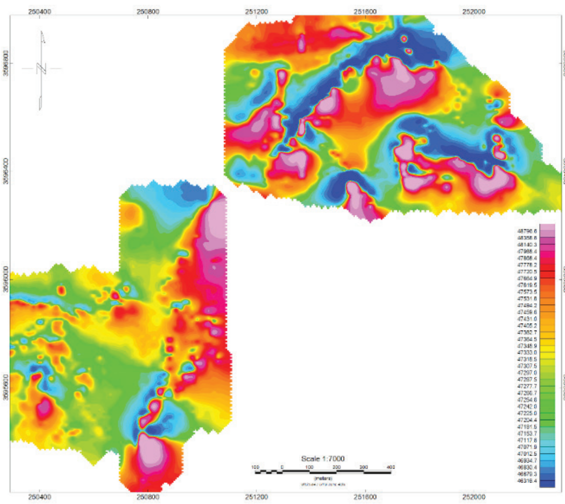

Figure 5. Magnetometric field map of whole range (TMI).

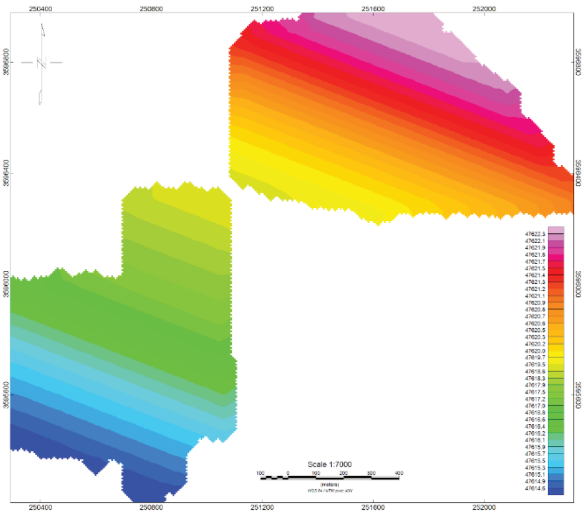

Figure 6. Map of magnetic field of whole Earth (IGRF Effect) in the range.

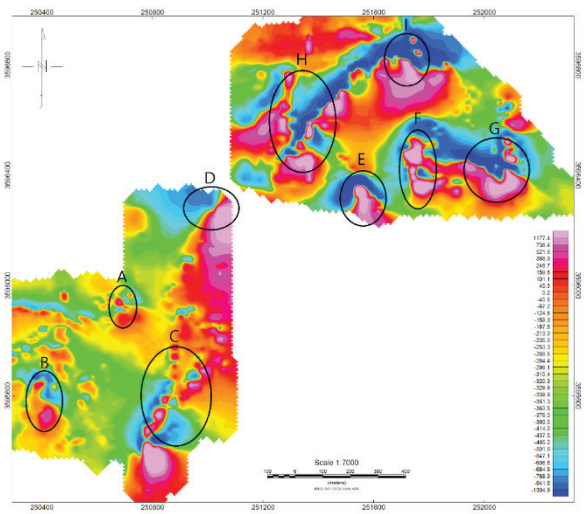

Figure 7. Total magnetic field map of range after removing IGRF effect.

Terrestrial Magnetometric Data Processing

After preparing the total magnetic field map of the area, and after removing the IGRF effect, it is necessary to perform the processing of this data. The first step in processing data is to apply a polarization filter. The polarisation filter or converter transmits the magnetic field from a magnetic latitude at which the Earth's magnetic field vector is inclined to the magnetic pole, where the magnetic field is vertical. As a result of applying this filter, the asymmetric shape of the magnetic anomaly is converted to a symmetrical shape concerning the source that creates it, causing the anomaly to be correctly located on the deposit mass and determining its slope. The map obtained by applying the polarization filter on the entire magnetic field map is presented in Figure 8 after removing the IGRF effect. According to the map, besides the maxima and minima that can be seen on the map, it can be said that anomalies A, B and C have a slope to the north, anomaly D to the northwest, and anomalies E, F, G, H and I have a slope to the northeast.

The nature of magnetic anomalies is bipolar and the origin of the anomaly is located approximately in the middle of these two poles. This phenomenon is one of the factors complicating the interpretation of magnetic maps. To solve this problem, a reduction to the pole filter (RTP) is provided. At the North Pole, the magnetic vector enters the Earth vertically, which causes the positive pole to grow and be located just above its originator, and the negative pole to decompose and move to anomalous margins. Due to the presence of the magnetic dipole, the anomalous position with the maximum values cannot indicate the position of the anomalous mass on the Earth's surface. For this purpose, the residual map was reducted to the pole, taking into account the deviation angle of 2.9 degrees and the inclination angle of 50 degrees for this area.

Then, the surface trend filter was used. This filter is used to obtain the remaining anomaly. This method uses the fitting of polynomials with different degrees on the measured data. The principle of this filter is based on a surface that has the best compliance with the measured values. This level is considered as regional effects. The remaining magnetic anomalies are obtained after subtracting these values from the observation data. This filter was applied to the polarisation magnetic field map. The residual anomaly maps resulting from the trends (levels) in grades 1 to 3 are shown in Figures 9, 10 and 11.

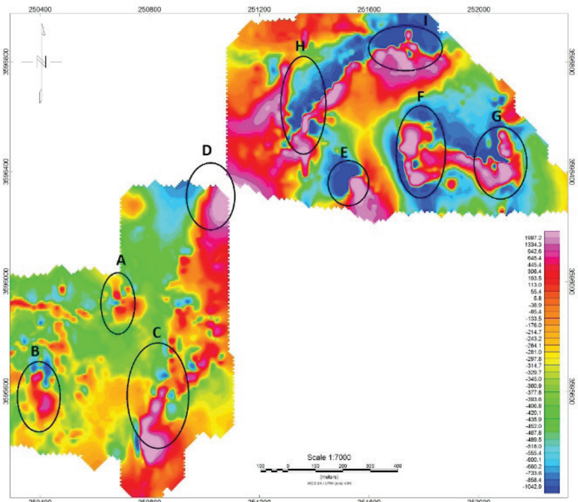

Figure 8. Total magnetic field map after applying polarization filter.

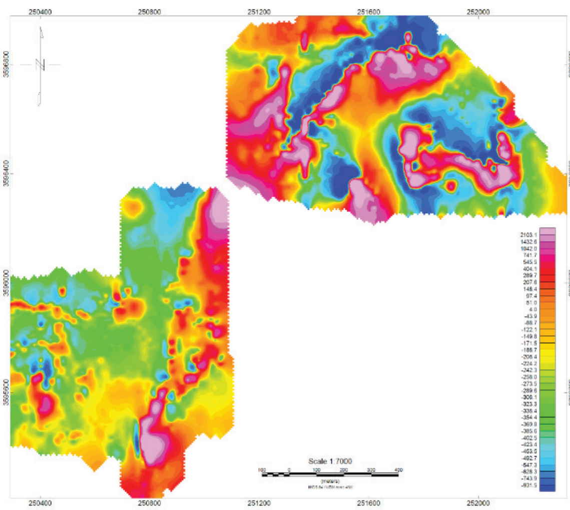

Figure 9. Residual anomaly maps resulting from elimination of first-order surface trend.

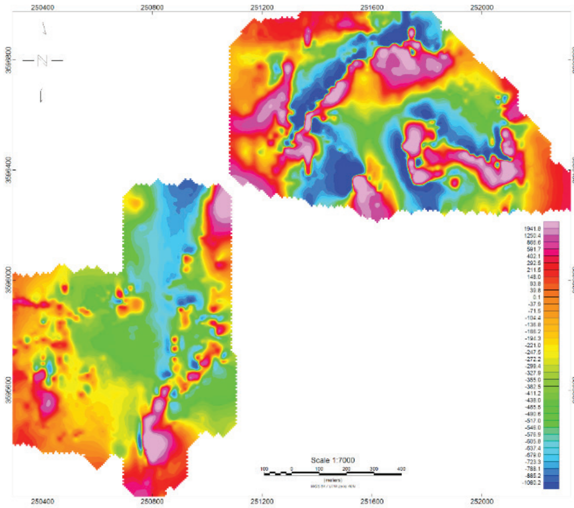

Figure 10. Remaining anomaly maps resulting from elimination of quadratic surface trend.

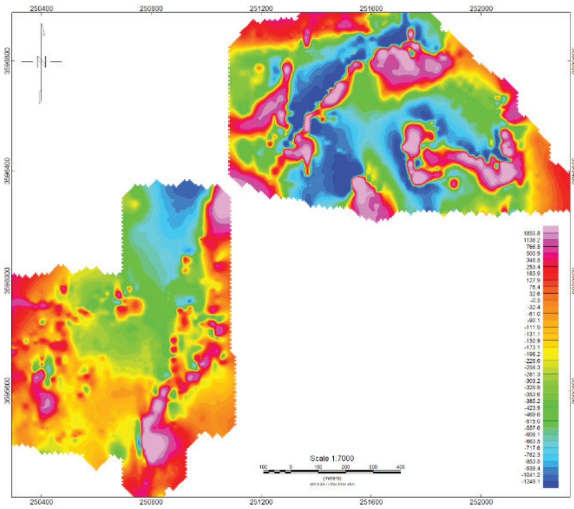

Figure 11. Remaining anomaly maps resulting from elimination of third-degree surface trend.

According to the resulting maps, which are not very different and only the expansion of the minima and maxima is slightly different, the area anomalies can be adapted to the map resulting from eliminating the first-order surface trend; because it is more consistent with the rest of the results. Therefore, this map can be used to interpret and diagnose the remaining anomalies.

The first-degree surface trend map is in full compliance with geological formations such as lithology units and faults. Therefore, the first-degree surface trend was used in the interpretation and diagnosis of residual anomalies. Applying the upward continuation filter is the next step in the data processing. Separating local anomalies from regional ones is one of the essential tasks in processing and analyzing magnetic data. The upward continuation process is a mathematical transformation of the measured data that attenuates anomalies with short wavelengths. In other words, the upward continuation filter weakens the effect of superficial anomalies. Therefore, it can be used as a suitable tool to separate short-wavelength local anomalies from long-wavelength regional anomalies. In the upward continued filtration method, it is essential to choose the optimal height of the field; because a height less than the optimal value causes the remaining effect of local anomalies in the data, and in contrast, a height higher than the optimal value causes a double attenuation effect of regional anomalies in the data. Upward continued filtration is applied to the data of the Kahrang range for altitudes from zero to 200 meters, with a step of 10 meters on the polarisation map of the Kahrang range. Some upward continued filtration maps are shown in Figures 12 and 13. According to these maps, local anomalies in this area are highly magnetic in the centre of the range; they also show a low value in the northeast and southwest of the area and can be considered local anomalies.

According to the above figures, there are not many changes in the exploration area of the northeastern region, and when the change in height is more than 90 meters, the anomalous effect of the areas becomes more evident.

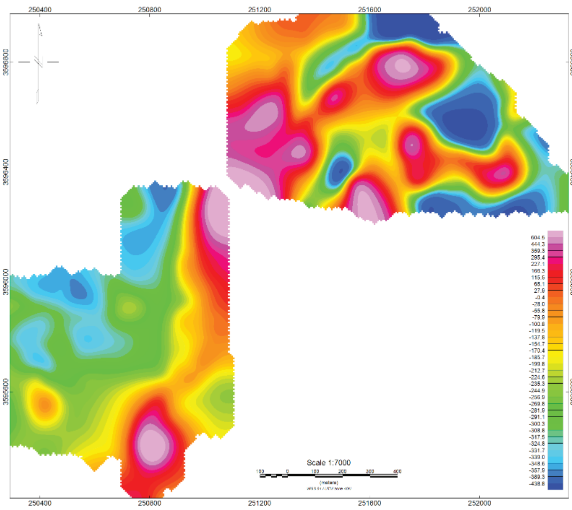

Figure 12. Upward extension, 50 m.

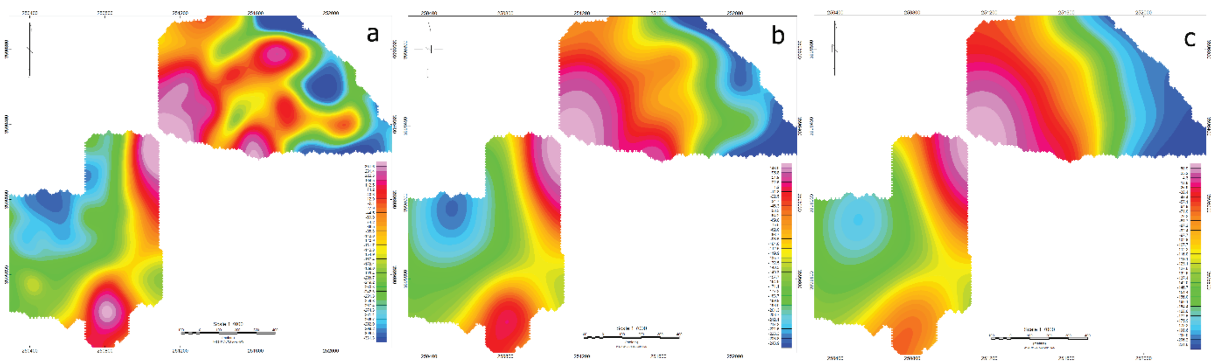

Figure 13. Upward extension of **a)** 90 meters, **b)** 200 meters, **c)** 300 meters.

Then, a vertical derivative filter was applied. The vertical derivative filter is one of the essential tools in determining the edges of anomalies and the boundaries of geological zones. This filter was also applied to the polarisation magnetic field map. Vertical derivative maps of the first and second-order were also prepared. The second-order derivative was omitted due to high noise. Figure 14 shows the vertical derivative of first-order. As seen in the first-order vertical derivative map, surface anomalies and noise levels are low, and the range of anomalies is somewhat well defined and their boundaries well defined. However, in the second-order vertical derivative map, noise and turbulence have increased, and it is impossible to separate the anomalies.

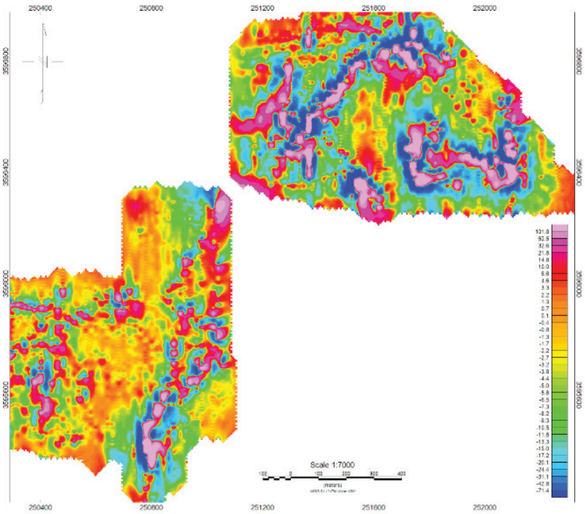

Figure 14. Map of applying first-order vertical derivative filter on range data.

In the last step, an analytical signal filter was applied to the data. This filter is entirely independent of the rocks' magnetization direction and the Earth's magnetic field. As a result, each object with the same geometrical properties has the same analytical signal. The peak of this filter is usually located directly above the edge of wide objects and above the centre of narrow objects. As a result, the geometry of magnetic masses can be mainly understood with this filter. This filter is applied to the polarisation magnetic field map. The analytical signal map is shown in Figure 15. As can be seen, the maximum values on this map are seen in the northeast, southwest and centre. By comparing the analytical signal map with the polarisation filter map, it appears that the anomalies F, G, H, and I are continuous in the northeast.

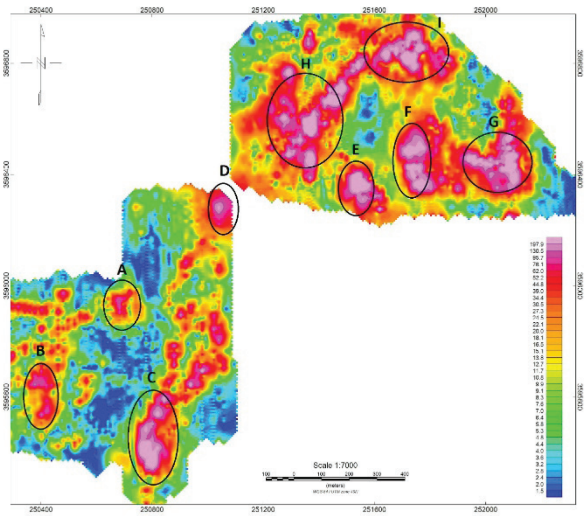

Figure 15. Map resulting from application of analytical signal filters on regional data.

Based on the obtained shapes, it can be said that the processing performed on the terrestrial magnetometric data by the polarisation filters method, surface trend filter, upward continuation, vertical derivative, and analytical signal method led to the discovery of anomalies A to I in the two desired Exploration area. Due to the homogeneous dipoles in the remaining magnetic map, iron mineralization probability (possibility) in this range is high. From the upward continuation derivative on the magnetic map, the remaining base anomalies were approximately identified.

CONCLUSION

This section summarises the results of the conducted research in the study area:

After removing the effect of IGRF in the terrestrial magnetometric data, it was found that the Exploration area has several peaks in the southwestern and northeastern regions of the range. These anomalies correspond to igneous rock units (rhyolites) and faults in the area.

Applying a polarization filter on the terrestrial magnetometric data determined that anomalies A, B and C slope in the northern direction and anomaly D in the northwest direction. The anomalies E, F, G and H, and H and I, slope to the northeast.

Applying an analytical signal filter on the terrestrial magnetometric data determined that the anomalies F, G, H, and I are continuous in the northeast.

Applying the upward continuation filter on the terrestrial magnetometric data determined that the anomalies are concentrated in the centre part of the area. In the northeast and southwest part, the area of anomalies is local.

According to the geological map of the area and the anomalies identified in the reduction to the pole (RTP) map, a close relationship between mineralization and faults can be found in the northeast of the area. Also, the relationship between lithology units and the occurrence of magnetite vein samples on the surface has been interpreted, and anomalies identified in the southwest of the area.

ORCID

Ali Akbar Aali https://orcid.org/0000-0001-7420-5525
Aref Shirazi https://orcid.org/0000-0001-7623-301X
Adel Shirazy https://orcid.org/0000-0001-7756-3205
Shayan Khakmardan https://orcid.org/0000-0003-4359-9538
Abbas Maghsoudi https://orcid.org/0000-0003-1683-9209
Ardeshir Hezarkhani https://orcid.org/0000-0002-1149-3440

REFERENCES

Abubakar, R., Muxworthy, A., Sephton, M., Southern, P., Watson, J., Fraser, A., & Almeida, T. (2015). Formation of magnetic minerals at hydrocarbon-generation conditions. *Marine and Petroleum Geology*, *68*, 509-519.

Alahgholi, S., Shirazy, A., & Shirazi, A. (2018). Geostatistical studies and anomalous elements detection, Bardaskan Area, Iran. *Open Journal of Geology*, *8*(7), 697-710.

Bao-xian, Y. (2013). Data sharing between different proton magnetometer [J]. *Inner Mongolia Coal Economy*, *5*.

Chelotti, L., Acosta, N., & Foster, M. (2009). Cátedra de Geofísica Aplicada. *Universidad Nacional de la Patagonia San Juan Bosco, Argentina*.

Company, K. (2016). *Gravimetric studies and combining the results with magnetometric studies of the Hoz Vali iron ore range*.

Company, Y. Z. Y. M. C. (2018). *Kahrang Iron Ore Mine Exploration Report*.

Currenti, G., Napoli, R., Carbone, D., Del Negro, C., & Ganci, G. (2007). Inverse modeling in geophysical applications. In *Applied And Industrial Mathematics In Italy II* (pp. 279-290). World Scientific.

Dobrin, M. B., & Savit, C. (1988). *Introduction to Geophysical Prospecting*. McGraw-Hill Book Co. New York.

Doodran, R. J., Khakmardan, S., Shirazi, A., & Shirazy, A. (2020). Minimalization of Ash from Iranian Gilsonite by Froth Flotation. *Journal of Minerals and Materials Characterization and Engineering*, *9*(1), 1-13.

Edelstein, A. (2007). Advances in magnetometry. *Journal of Physics: Condensed Matter*, *19*(16), 165217.

Ghorbani, M. (2013a). *Economic geology of Iran* (Vol. 581). Springer.

Ghorbani, M. (2013b). A summary of geology of Iran. In *The economic geology of Iran* (pp. 45-64). Springer.

Khakmardan, S., Doodran, R. J., Shirazy, A., Shirazi, A., & Mozaffari, E. (2020). Evaluation of Chromite Recovery from Shaking Table Tailings by Magnetic Separation Method. *Open Journal of Geology*, *10*(12), 1153-1163.

Khakmardan, S., Shirazi, A., Shirazy, A., & Hosseingholi, H. (2018). Copper oxide ore leaching ability and cementation behavior, mesgaran deposit in Iran. *Open Journal of Geology*, *8*(09), 841.

Khayer, K., Shirazy, A., Shirazi, A., Ansari, A., Nazerian, H., & Hezarkhani, A. (2021). Determination of Archie's Tortuosity Factor from Stoneley Waves in Carbonate Reservoirs. *International Journal of Science and Engineering Applications (IJSEA)*, *10*, 107-110.

Khosravi, V., Shirazi, A., Shirazy, A., Hezarkhani, A., & Pour, A. B. (2022). Hybrid Fuzzy-Analytic Hierarchy Process (AHP) Model for Porphyry Copper Prospecting in Simorgh Area, Eastern Lut Block of Iran. *Mining*, *2*(1), 1-12.

Liu, H., Dong, H., Liu, Z., Ge, J., Bai, B., & Zhang, C. (2017). Construction of an Overhauser magnetic gradiometer and the applications in geomagnetic observation and ferromagnetic target localization. *Journal of Instrumentation*, *12*(10), T10008.

Minshull, T. (2003). Kearey, P., Brooks, M. & Hill, I. 2002. An Introduction to Geophysical Exploration, ix+262 pp. Oxford: Blackwell Science. *Geological Magazine*, *140*(3), 366-366.

Nabighian, M. N., Grauch, V., Hansen, R., LaFehr, T., Li, Y., Peirce, J. W., Phillips, J. D., & Ruder, M. (2005). The historical development of the magnetic method in exploration. *Geophysics*, *70*(6), 33ND-61ND.

Shirazi, A., Hezarkhani, A., Shirazy, A., & Shahrood, I. (2018a). Exploration Geochemistry Data-Application for Cu Anomaly Separation Based On Classical and Modern Statistical Methods in South Khorasan, Iran. *International Journal of Science and Engineering Applications*, *7*, 39-44.

Shirazi, A., Hezarkhani, A., Shirazy, A., & Shahrood, I. (2018b). Remote sensing studies for mapping of iron oxide regions, South of Kerman, Iran. *International Journal of Science and Engineering Applications*, *7*(4), 45-51.

Shirazi, A., Shirazy, A., & Karami, J. (2018c). Remote sensing to identify copper alterations and promising regions, Sarbishe, South Khorasan, Iran. *International Journal of Geology and Earth Sciences*, *4*(2), 36-52.

Shirazi, A., Shirazy, A., Saki, S., & Hezarkhani, A. (2018d). Geostatistics studies and geochemical modeling based on core data, sheytoor iron deposit, Iran. *Journal of Geological Resource and Engineering*, *6*, 124-133.

Shirazy, A., Shirazi, A., Heidarlaki, S., & Ziaii, M. (2018a). Exploratory Remote Sensing Studies to Determine the Mineralization Zones around the Zarshuran Gold Mine. *International Journal of Science and Engineering Applications*, *7*(9), 274-279.

Shirazy, A., Shirazi, A., & Hezarkhani, A. (2018b). Predicting gold grade in Tarq 1: 100000 geochemical map using the behavior of gold, Arsenic and Antimony by K-means method. *Journal of Mineral Resources Engineering*, *2*(4), 11-23.

Shirazy, A., Shirazi, A., Ferdossi, M. H., & Ziaii, M. (2019). Geochemical and geostatistical studies for estimating gold grade in tarq prospect area by k-means clustering method. *Open Journal of Geology*, *9*(6), 306-326.

Shirazy, A., Ziaii, M., & Hezarkhani, A. (2020a). Geochemical Behavior Investigation Based on K-means and Artificial Neural Network Prediction for Copper, in Kivi region, Ardabil province, Iran. *Iranian Journal of Mining Engineering*, *14*(45), 96-112.

Shirazy, A., Ziaii, M., Hezarkhani, A., & Timkin, T. (2020b). Geostatistical and remote sensing studies to identify high metallogenic potential regions in the Kivi area of Iran. *Minerals*, *10*(10), 869.

Shirazy, A., Hezarkhani, A., Timkin, T., & Shirazi, A. (2021a). Investigation of Magneto-/Radio-Metric Behavior in Order to Identify an Estimator Model Using K-Means Clustering and Artificial Neural Network (ANN) (Iron Ore Deposit, Yazd, Iran). *Minerals*, *11*(12), 1304.

Shirazy, A., Shirazi, A., & Nazerian, H. (2021b). Application of Remote Sensing in Earth Sciences–A Review. *International Journal of Science and Engineering Applications*, *10*, 45-51.

Shirazy, A., Shirazi, A., Nazerian, H., & Hezarkhani, A. (2021c). Investigation of Geochemical Sections in Exploratory Boreholes of Mesgaran Copper Deposit in Iran. *International Journal for Research in Applied Science and Engineering Technology (IJRASET)*, *9*(8), 2364-2368.

Shirazy, A., Shirazi, A., Nazerian, H., Khayer, K., & Hezarkhani, A. (2021d). Geophysical study: Estimation of deposit depth using gravimetric data and Euler method (Jalalabad iron mine, Kerman province of Iran). *Open Journal of Geology*, *11*(8), 340-355.

Shirazy, A., Ziaii, M., & Hezarkhani, A. (2021e). Geochemical behavior investigation based on k-means and artificial neural network prediction for titanium and zinc, Kivi region, Iran. *Bulletin of the Tomsk Polytechnic University, Geo Assets Engineering*, *332*(3), 113-125.

Shirazy, A., Hezarkhani, A. , Shirazi, A. , Khakmardan, S. & Rooki, R. (2022). K-Means Clustering and General Regression Neural Network Methods for Copper Mineralization probability in Chahar-Farsakh, Iran. *Geological Bulletin of Turkey*, *65*(1), 79-92. https://doi.org/10.25288/tjb.1010636

Spaldin, N. A. (2010). *Magnetic materials: fundamentals and applications*. Cambridge University press.

Tian, W.-f., Hao, J.-J., Yan, J.-y., Li, C.-z., & Zhao, X.-w. (2010). Application of synthetic geophysical methods to deep exploration of Hanxing-type iron deposit. *Progress in Geophysics*, *25*(4), 1442-1452.